

# Quantum dissipation with nonlinear environment couplings: Stochastic fields dressed dissipaton equation of motion approach

Zi-Hao Chen,<sup>1,\*</sup> Yao Wang,<sup>2,\*</sup> Rui-Xue Xu,<sup>1,2,3,†</sup> and YiJing Yan<sup>1,2,3,‡</sup>

<sup>1</sup>*Department of Chemical Physics, University of Science and Technology of China, Hefei, Anhui 230026, China*

<sup>2</sup>*Hefei National Laboratory for Physical Sciences at the Microscale,*

*University of Science and Technology of China, Hefei, Anhui 230026, China*

<sup>3</sup>*iChEM and Synergetic Innovation Center of Quantum Information and Quantum Physics,*

*University of Science and Technology of China, Hefei, Anhui 230026, China*

(Dated: October 6, 2021)

Accurate and efficient simulation on quantum dissipation with nonlinear environment couplings remains nowadays a challenging task. In this work, we propose to incorporate the stochastic fields, which resolve just the nonlinear environment coupling terms, into the dissipaton–equation–of–motion (DEOM) construction. The stochastic fields are introduced via the Hubbard–Stratonovich transformation. After the transformation, the resulted stochastic–fields–dressed total Hamiltonian contains only linear environment coupling terms. On basis of that, a stochastic–fields–dressed DEOM (SFD–DEOM) can then be constructed. The resultant SFD–DEOM, together with the ensemble average over the stochastic fields, constitutes an exact and nonperturbative approach to quantum dissipation under nonlinear environment couplings. It is also of relatively high efficiency and stability due to the fact that only nonlinear environment coupling terms are dealt with stochastic fields while linear couplings are still treated as the usual DEOM. Numerical performance and demonstrations are presented with a two-state model system.

## I. INTRODUCTION

Quantum dissipation is pivotal in many fields of modern science. The underlying non-Markovian and nonperturbative quantum nature would be prominent whenever the system and its embedded environment are highly correlated. Various approaches have been proposed, focusing on the reduced dynamics of system under the influence of bath. Exact theories under Gaussian baths include the Feynman–Vernon influence functional method,[1–3] and its differential equivalence, the hierarchical–equations–of–motion (HEOM) formalism.[4–8] Adopting dissipatons as quasi-particles to characterize the interacting bath statistical properties, a dissipaton–equation–of–motion (DEOM) theory has been constructed.[9–12] The DEOM not only recovers the HEOM for the reduced system dynamics, but also is convenient to treat the hybridized bath dynamics and polarizations.[13, 14]

All these theories exploit the Gaussian thermodynamic statistics, making them strictly valid only for the linear coupling harmonic bath. Without loss of generality, let us consider single dissipative mode cases. The total system–plus–bath composite Hamiltonian takes the form,  $H_{\text{T1}} = H_{\text{S}} + h_{\text{B}} + \hat{Q}_{\text{S}}(\alpha_0 + \alpha_1 \hat{x}_{\text{B}})$ . The system Hamiltonian  $H_{\text{S}}$  and dissipative mode operator  $\hat{Q}_{\text{S}}$  are arbitrary, whereas the bath Hamiltonian and solvation coordinate assume  $h_{\text{B}} = \frac{1}{2} \sum_j \omega_j (\hat{p}_j^2 + \hat{q}_j^2)$  and  $\hat{x}_{\text{B}} = \sum_j c_j \hat{q}_j$ . In this paper, we set  $\hat{Q}_{\text{S}}$  and  $\hat{x}_{\text{B}}$  be dimensionless. The  $\alpha$ -parameters are then of energy unit. Involved here are only  $\alpha_0$ -term and  $\alpha_1$ -term, without higher-order terms.

This linearity intrinsically implies a weak backaction of the central system on the bath.

On the other hand, nonlinear couplings are often inevitable in real systems and crucial in related processes. For example, the quadratic noise fluctuations can become the dominant source of decoherence in designing quantum computing devices.[15–18] Quadratic couplings are also closely associated with the Duschinsky rotation in studying optical spectroscopies and rate problems of molecular systems.[19–24] Although there have been theoretically a few attempts to the quantum dissipative dynamics under nonlinear bath coupling influences,[25–30] the quest of an exact quantum dissipation theory plus an efficient numerical method remains in general a challenging task.

This paper focuses on quadratic bath coupling cases which lead to the total Hamiltonian  $H_{\text{T}} = H_{\text{T1}} + \hat{Q}_{\text{S}} \cdot \alpha_2 \hat{x}_{\text{B}}^2$  being of the form

$$H_{\text{T}} = H_{\text{S}} + h_{\text{B}} + \hat{Q}_{\text{S}}(\alpha_0 + \alpha_1 \hat{x}_{\text{B}} + \alpha_2 \hat{x}_{\text{B}}^2). \quad (1)$$

This form of total Hamiltonian can be brought out on basis of a widely adopted microscopic electron/exciton transfer model containing Duschinsky rotation.[25, 26] The involving bath coupling descriptors,  $\{\alpha_n; n = 0, 1, 2\}$ , are found interconnected and shall be seriously determined to satisfy basic physical requirements. This issue has been elaborated in our previous work.[26] Meanwhile by extending the dissipaton algebra to dissipaton-pair actions, an Ehrenfest mean-field type of DEOM approach has been constructed there for quadratic bath couplings.[25, 26]

In this work, we propose a new method to tackle the nonlinear coupling term via stochastic fields, induced by the Hubbard–Stratonovich (HS) transformation,[31–33] and then enrolled into the construction of DEOM. Note that for the stochastic–fields–dressed (SFD) DEOM (SFD–DEOM) method to be developed, the extension to

\*Authors of equal contributions

†Electronic address: rxxu@ustc.edu.cn

‡Electronic address: yanyj@ustc.edu.cn

include higher-order  $\hat{x}_B^n$ -coupling terms are straightforward. Actually in principle, the scenario can be applied to the total Hamiltonian being of the form  $H_{\text{Total}} = H_S + h_B + \sum_a \hat{Q}_a \hat{F}_a^{n_a}$ , where  $\{\hat{Q}_a\}$  and  $\{\hat{F}_a; \hat{F}_a = \sum_j c_{aj} \hat{q}_j\}$  are system and bath operators, respectively, and the integers  $n_a \geq 0$ . The resultant SFD-DEOM, together with the ensemble average over stochastic fields, constitutes an exact and nonperturbative approach for quantum dissipation with nonlinear bath couplings. The paper is arranged as follows. Theoretical constructions are made in Sec. II, with HS transformation in Sec. II A, SFD-DEOM construction in Sec. II B, and a norm conserved propagation via Girsanov transformation (GT) in Sec. II C. Numerical demonstrations are given in Sec. III and the paper is summarized in Sec. IV. Throughout the paper, we set  $\hbar = 1$  and  $\beta = 1/(k_B T)$ .

## II. THEORY

### A. HS transformation and SFD Hamiltonian

According to the total composite Hamiltonian in Eq. (1), the total propagator can be recast as

$$U(t) \equiv e^{-iH_T t} = \lim_{N_t \rightarrow \infty} \prod_{i=1}^{N_t} e^{-iH_{T1} \Delta t} e^{-i\alpha_2 \hat{Q}_S \hat{x}_B^2 \Delta t}, \quad (2)$$

with  $\Delta t = t/N_t$ . Here, the nonlinear  $\alpha_2$ -term has been extracted out at each tiny propagating time step. Adopting the HS transformation,[31–33] it can be expressed in the form of

$$e^{-i\alpha_2 \hat{Q}_S \hat{x}_B^2 \Delta t} = \sqrt{\frac{\Delta t}{2\pi}} \int d\xi e^{-\frac{\Delta t}{2} \xi^2} e^{(1-i)\xi \sqrt{\alpha_2} \hat{Q}_S^{\frac{1}{2}} \hat{x}_B \Delta t}. \quad (3)$$

Thus, the propagator in Eq.(2) can now be obtained as the ensemble average over the HS-transformation induced stochastic field,  $\xi_t$ , as

$$U(t) = \mathcal{M}_{\xi_t} \{ \tilde{U}(t; \xi_t) \}, \quad (4)$$

with the SFD propagator

$$\tilde{U}(t; \xi_t) = \lim_{N_t \rightarrow \infty} \prod_{i=1}^{N_t} e^{-i\tilde{H}_T(\xi_t) \Delta t}, \quad (5)$$

and  $\mathcal{M}_{\xi_t}$  denoting the ensemble average over the real stochastic field,  $\xi_t$ . In Eq.(5), the SFD Hamiltonian reads

$$\tilde{H}_T(\xi_t) = H_0 + h_B + \tilde{Q}_S(\xi_t) \hat{x}_B, \quad (6)$$

with  $H_0 = H_S + \alpha_0 \hat{Q}_S$  and

$$\tilde{Q}_S(\xi_t) = \alpha_1 \hat{Q}_S + (1+i)\xi_t \sqrt{\alpha_2} \hat{Q}_S^{\frac{1}{2}}. \quad (7)$$

Similarly, the inverse propagator can be recast as

$$U^\dagger(t) = \mathcal{M}_{\xi'_t} \{ \tilde{U}^\dagger(t; \xi'_t) \}, \quad (8)$$

where

$$\tilde{U}^\dagger(t; \xi'_t) = \lim_{N_t \rightarrow \infty} \prod_{i=1}^{N_t} e^{i\tilde{H}_T^\dagger(\xi'_t) \Delta t}, \quad (9)$$

with

$$\tilde{H}_T^\dagger(\xi'_t) = H_0 + h_B + \tilde{Q}_S^\dagger(\xi'_t) \hat{x}_B, \quad (10)$$

and

$$\tilde{Q}_S^\dagger(\xi'_t) = \alpha_1 \hat{Q}_S + (1-i)\xi'_t \sqrt{\alpha_2} \hat{Q}_S^{\frac{1}{2}}. \quad (11)$$

Note that extensions to higher-order bath couplings can just be done via multiple HS transformations in a recursive manner.

On basis of the above elaborations [cf. Eqs. (4) and (8)], the total density operator at time  $t$  can be expressed as

$$\rho_T(t) = U(t) \rho_T(0) U^\dagger(t) = \mathcal{M}_{\xi_t, \xi'_t} \{ \tilde{\rho}_T(t; \xi_t, \xi'_t) \}, \quad (12)$$

with

$$\tilde{\rho}_T(t; \xi_t, \xi'_t) = \tilde{U}(t; \xi_t) \rho_T(0) \tilde{U}^\dagger(t; \xi'_t) \equiv \tilde{\rho}_T(t), \quad (13)$$

which leads to the reduced system density operator,  $\rho_S(t) \equiv \text{tr}_B[\rho_T(t)]$ , the following form

$$\rho_S(t) = \mathcal{M}_{\xi_t, \xi'_t} \{ \tilde{\rho}_S^\circ(t; \xi_t, \xi'_t) \}, \quad (14)$$

where  $\tilde{\rho}_S^\circ(t; \xi_t, \xi'_t) \equiv [\tilde{\rho}_S(t) + \tilde{\rho}_S^\dagger(t)]/2$  with

$$\tilde{\rho}_S(t; \xi_t, \xi'_t) = \text{tr}_B[\tilde{\rho}_T(t; \xi_t, \xi'_t)] \equiv \tilde{\rho}_S(t). \quad (15)$$

For brevity in later use, we have denoted  $\tilde{\rho}_T(t)$  and  $\tilde{\rho}_S(t)$  for  $\tilde{\rho}_T(t; \xi_t, \xi'_t)$  and  $\tilde{\rho}_S(t; \xi_t, \xi'_t)$  in Eq.(13) and Eq.(15), respectively. Involved in the SFD total Hamiltonians, Eqs.(6) and (10), are only linear bath couplings. The standard DEOM construction[9–11] can thus be applied to the evolution of  $\tilde{\rho}_S(t)$ , with the total Hamiltonians being Eqs.(6) and (10) for the left and right actions, respectively. The reduced system evolution  $\rho_S(t)$  is then obtained via ensemble average over the stochastic fields.

### B. SFD-DEOM construction

We are now in the position to derive the SFD-DEOM. Let us start from the exponential series expansion on the bath correlation function, which serves as the common setup for constructing DEOM/HEOM formalisms. This expansion is based on the fluctuation-dissipation theorem,[3] reading

$$\langle \hat{x}_B^B(t) \hat{x}_B^B(0) \rangle_B = \frac{1}{\pi} \int_{-\infty}^{\infty} d\omega \frac{e^{-i\omega t} J_B(\omega)}{1 - e^{-\beta\omega}}, \quad (16)$$

with  $\hat{x}_B^B(t) \equiv e^{ih_B t} \hat{x}_B e^{-ih_B t}$  and the average  $\langle \cdot \rangle_B \equiv \text{tr}_B[\cdot e^{-\beta h_B}] / \text{tr}_B(e^{-\beta h_B})$  both defined in the bare-bath subspace. The involved hybridization bath spectral density  $J_B(\omega)$  in Eq.(16) is given by[3]

$$J_B(\omega) = \frac{1}{2} \int_{-\infty}^{\infty} dt e^{i\omega t} \langle [\hat{x}_B^B(t), \hat{x}_B^B(0)] \rangle_B. \quad (17)$$

It satisfies  $J_B(-\omega) = -J_B(\omega)$ . The exponential series expansion on Eq. (16) can be achieved by adopting a certain sum-over-poles scheme to expand the Fourier integrand, followed by Cauchy's contour integration. Together with the time-reversal relation  $\langle \hat{x}_B^{\text{B}}(0) \hat{x}_B^{\text{B}}(t) \rangle_B = \langle \hat{x}_B^{\text{B}}(t) \hat{x}_B^{\text{B}}(0) \rangle_B^*$ , the expansion form of bath correlation function for  $t \geq 0$  is obtained as[9–11]

$$\begin{aligned} \langle \hat{x}_B^{\text{B}}(t) \hat{x}_B^{\text{B}}(0) \rangle_B &= \sum_{k=1}^K \eta_k e^{-\gamma_k t}, \\ \langle \hat{x}_B^{\text{B}}(0) \hat{x}_B^{\text{B}}(t) \rangle_B &= \sum_{k=1}^K \eta_k^* e^{-\gamma_k t}. \end{aligned} \quad (18)$$

The second expression is due to the fact that  $\{\gamma_k\}$  must be either real or complex-conjugate paired. The associated index  $\bar{k} \in \{k = 1, \dots, K\}$  is defined via  $\gamma_{\bar{k}} \equiv \gamma_k^*$ .

Dissipatons, with coordinates  $\{\hat{f}_k\}$ , [12] can now be introduced as statistically independent quasi-particles via

$$\hat{x}_B = \sum_{k=1}^K \hat{f}_k, \quad (19)$$

with  $\hat{f}_k(t) \equiv e^{ih_B t} \hat{f}_k e^{-ih_B t}$  and

$$\begin{aligned} \langle \hat{f}_k(t) \hat{f}_{k'}(0) \rangle_B &= \delta_{kk'} \eta_k e^{-\gamma_k t}, \\ \langle \hat{f}_{k'}(0) \hat{f}_k(t) \rangle_B &= \delta_{kk'} \eta_k^* e^{-\gamma_k t}. \end{aligned} \quad (20)$$

Obviously, Eq. (18) is reproduced. Similar to original DEOM formalism, dynamical variables in SFD-DEOM are the SFD dissipaton-augmented-reduced density operators (SFD-DDOs):[9–11]

$$\tilde{\rho}_{\mathbf{n}}^{(n)}(t) \equiv \tilde{\rho}_{n_1 \dots n_K}^{(n)}(t) \equiv \text{tr}_B [(\hat{f}_K^{n_K} \dots \hat{f}_1^{n_1})^\circ \tilde{\rho}_T(t)]. \quad (21)$$

Here,  $n = n_1 + \dots + n_K$  and  $\mathbf{n} \equiv \{n_k; k = 1, \dots, K\}$ , with all  $n_k \geq 0$  for bosonic dissipatons. The product of dissipaton operators inside  $(\dots)^\circ$  is *irreducible*, satisfying  $(\hat{f}_k \hat{f}_j)^\circ = (\hat{f}_j \hat{f}_k)^\circ$  for boson bathp. Each  $n$ -particles SFD-DDO,  $\tilde{\rho}_{\mathbf{n}}^{(n)}(t)$ , is specified with an ordered set of indexes,  $\mathbf{n}$ . For later use, we denote also  $\mathbf{n}_k^\pm$  which differs from  $\mathbf{n}$  only at the specified  $\hat{f}_k$ -dissipaton participation number  $n_k$  by  $\pm 1$ . The reduced system SFD density operator is just  $\tilde{\rho}_{\mathbf{0}}^{(0)}(t) = \tilde{\rho}_{0 \dots 0}^{(0)}(t) = \tilde{\rho}_S(t)$ .

In Eq. (21), the  $\tilde{\rho}_T(t)$ , as defined in Eq. (13), satisfies

$$\begin{aligned} \dot{\tilde{\rho}}_T(t) &= -i[\tilde{H}_T(\xi_t) \tilde{\rho}_T(t) - \tilde{\rho}_T(t) \tilde{H}_T^\dagger(\xi'_t)] \\ &= -i[H_0^\times + h_B^\times + \tilde{Q}_S^\times(\xi_t) \hat{x}_B^\times - \tilde{Q}_S^{\dagger \times}(\xi'_t) \hat{x}_B^{\times \dagger}] \tilde{\rho}_T(t), \end{aligned} \quad (22)$$

where  $\hat{A}^\times \equiv \hat{A}^> - \hat{A}^<$  and

$$\hat{A}^> \tilde{\rho}_T(t) \equiv \hat{A} \tilde{\rho}_T(t), \quad \hat{A}^< \tilde{\rho}_T(t) \equiv \tilde{\rho}_T(t) \hat{A}.$$

The SFD-DEOM for the time evolution of  $\tilde{\rho}_{\mathbf{n}}^{(n)}(t)$  is obtained by applying Eq. (22) to Eq. (21), followed by the standard procedure of deriving the general DEOM

formalism.[9–14] During that, key steps are the generalized Wick's theorem,[9–11]

$$\begin{aligned} \tilde{\rho}_{\mathbf{n}}^{(n)}(t; \hat{f}_k^>) &= \text{tr}_B [(\hat{f}_K^{n_K} \dots \hat{f}_1^{n_1})^\circ \hat{f}_k \tilde{\rho}_T(t)] \\ &= \tilde{\rho}_{\mathbf{n}_k^+}^{(n+1)}(t) + \sum_{k'} n_{k'} \langle \hat{f}_{k'}(0^+) \hat{f}_k \rangle_B \tilde{\rho}_{\mathbf{n}_{k'}}^{(n-1)}(t), \\ \tilde{\rho}_{\mathbf{n}}^{(n)}(t; \hat{f}_k^<) &= \text{tr}_B [(\hat{f}_K^{n_K} \dots \hat{f}_1^{n_1})^\circ \tilde{\rho}_T(t) \hat{f}_k] \\ &= \tilde{\rho}_{\mathbf{n}_k^+}^{(n+1)}(t) + \sum_{k'} n_{k'} \langle \hat{f}_k \hat{f}_{k'}(0^+) \rangle_B \tilde{\rho}_{\mathbf{n}_{k'}}^{(n-1)}(t), \end{aligned}$$

and the generalized diffusion equation,[9–11]

$$\begin{aligned} \text{tr}_B [(ih_B^\times \hat{f}_k) \tilde{\rho}_T(t)] &= \text{tr}_B \left[ \left( \frac{\partial}{\partial t} \hat{f}_k \right)_B \tilde{\rho}_T(t) \right] \\ &= -\gamma_k \text{tr}_B [\hat{f}_k \tilde{\rho}_T(t)]. \end{aligned}$$

The final SFD-DEOM is obtained as

$$\begin{aligned} \dot{\tilde{\rho}}_{\mathbf{n}}^{(n)} &= -(iH_0^\times + \sum_k n_k \gamma_k) \tilde{\rho}_{\mathbf{n}}^{(n)} \\ &\quad - i \sum_k [\tilde{Q}_S^>(\xi_t) - \tilde{Q}_S^{\dagger <}(\xi'_t)] \tilde{\rho}_{\mathbf{n}_k^+}^{(n+1)} \\ &\quad - i \sum_k n_k [\eta_k \tilde{Q}_S^>(\xi_t) - \eta_k^* \tilde{Q}_S^{\dagger <}(\xi'_t)] \tilde{\rho}_{\mathbf{n}_k^-}^{(n-1)}. \end{aligned} \quad (23)$$

### C. Norm conserved propagation via GT

In principle, we can now propagate the SFD-DEOM on sampling and obtain the reduced system dynamics,  $\rho_S(t)$ , with respect to Eq. (14). However, direct implementation often easily causes instability and slow convergence. Further modification can be made by considering the norm conserved propagation. This can be done via the Girsanov transformation (GT).[33–36] Note that  $\xi_t$  and  $\xi'_t$  would be both white noises in the  $\Delta t \rightarrow 0$  limit. For white-noise-fields induced stochastic processes, the GT gives

$$\rho_S(t) = \mathcal{M}_{\xi_t, \xi'_t} [\tilde{\rho}_S^\circ(t; \xi_t, \xi'_t)] = \mathcal{M}_{\tilde{\xi}_t, \tilde{\xi}'_t} \left[ \frac{\tilde{\rho}_S^\circ(t; \tilde{\xi}_t, \tilde{\xi}'_t)}{\tilde{\Theta}(t; \tilde{\xi}_t, \tilde{\xi}'_t)} \right], \quad (24)$$

with

$$\tilde{\Theta}(t; \tilde{\xi}_t, \tilde{\xi}'_t) = \exp \left\{ \int_0^t d\tau \left[ \frac{\lambda_\tau^2}{2} - \lambda_\tau \tilde{\xi}_\tau + \frac{\lambda_\tau'^2}{2} - \lambda_\tau' \tilde{\xi}'_\tau \right] \right\}, \quad (25)$$

and

$$\lambda_t = \tilde{\xi}_t - \xi_t, \quad \lambda'_t = \tilde{\xi}'_t - \xi'_t. \quad (26)$$

In the following, we denote  $\tilde{\Theta}_t \equiv \tilde{\Theta}(t; \tilde{\xi}_t, \tilde{\xi}'_t)$  for convenience and choose

$$\tilde{\Theta}_t = \text{Re tr}_S [\tilde{\rho}_S(t; \tilde{\xi}_t, \tilde{\xi}'_t)], \quad (27)$$

for the norm conservation condition.

The problem now is to determine  $(\tilde{\xi}_t, \tilde{\xi}'_t)$  from  $(\xi_t, \xi'_t)$ . The stochastic fields entering Eq. (23) in computation

are then  $(\tilde{\xi}_t, \tilde{\xi}'_t)$  instead of  $(\xi_t, \xi'_t)$ . The reduced system density  $\rho_s(t)$  is then obtained via the second identity of Eq. (24) where  $\tilde{\rho}_s^\circ(t; \tilde{\xi}_t, \tilde{\xi}'_t) = [\tilde{\rho}_0^{(0)}(t; \tilde{\xi}_t, \tilde{\xi}'_t) + \text{h.c.}]/2$ . Firstly, for a single trajectory, we have, from Eq. (23), for  $\tilde{\Theta}_t$  of Eq. (27),

$$\begin{aligned} \dot{\tilde{\Theta}}_t/\tilde{\Theta}_t &= \text{Im} \left\{ \sum_k \text{tr}_s \left\{ [\tilde{Q}_s(\tilde{\xi}_t) - \tilde{Q}_s^\dagger(\tilde{\xi}'_t)] \tilde{\rho}_k^{(1)}(t) \right\} \right\} / \tilde{\Theta}_t \\ &\equiv \tilde{w}_t^- \tilde{\xi}_t + \tilde{w}_t^+ \tilde{\xi}'_t, \end{aligned} \quad (28)$$

where

$$\tilde{w}_t^\pm = \text{Re} \left\{ (1 \pm i) \sqrt{\alpha_2} \left\{ \sum_k \text{tr}_s [\tilde{Q}_s^{\frac{1}{2}} \tilde{\rho}_k^{(1)}(t)] \right\} \right\} / \tilde{\Theta}_t, \quad (29)$$

with

$$\tilde{\rho}_k^{(1)}(t) \equiv \text{tr}_B [\hat{f}_k \tilde{\rho}_T(t; \tilde{\xi}_t, \tilde{\xi}'_t)]. \quad (30)$$

Next, from Eq. (25), we have

$$\dot{\tilde{\Theta}}_t/\tilde{\Theta}_t = \frac{\lambda_t^2}{2} - \lambda_t \tilde{\xi}_t + \frac{\lambda_t'^2}{2} - \lambda_t' \tilde{\xi}'_t. \quad (31)$$

Comparing Eq. (28) with Eq. (31), we may set

$$\tilde{w}_t^- \tilde{\xi}_t = \frac{\lambda_t^2}{2} - \lambda_t \tilde{\xi}_t. \quad (32)$$

Substituting Eq. (26) into the above equation gives

$$\tilde{\xi}_t = \text{sgn}(\xi_t) \sqrt{\xi_t^2 + (\tilde{w}_t^-)^2} - \tilde{w}_t^-. \quad (33)$$

Here  $\text{sgn}(\cdot)$  is the sign function. The result of  $\tilde{\xi}'_t$  can be obtained similarly. The transformation of stochastic fields  $(\tilde{\xi}_t, \tilde{\xi}'_t)$  from  $(\xi_t, \xi'_t)$  for norm-conserved trajectory propagation is thus resolved. In numerical implementations both the originally generated stochastic fields  $\xi_t$  and  $\xi'_t$  and the GT resulted  $\tilde{\xi}_t$  and  $\tilde{\xi}'_t$  would then all be real.

We have thus finished the whole establishment of SFD-DEOM approach. In the norm conserved propagation, the stochastic fields entering the SFD-DEOM, Eq. (23), would be  $\tilde{\xi}_t$  and  $\tilde{\xi}'_t$ . The work flow can be outlined as follows.

- (1) Generate two real random numbers for  $\xi_t$  and  $\xi'_t$  according to the Gaussian distribution centered at 0 with the width  $1/\sqrt{\Delta t}$ ;
- (2) Perform GT to obtain  $\tilde{\xi}_t$  and  $\tilde{\xi}'_t$ ;
- (3) Get  $\tilde{Q}_s(\tilde{\xi}_t)$  and  $\tilde{Q}_s^\dagger(\tilde{\xi}'_t)$  via Eqs. (7) and (11), respectively, noting that  $\tilde{Q}_s^\dagger(\tilde{\xi}'_t) \neq [\tilde{Q}_s(\tilde{\xi}_t)]^\dagger$  since they involve different fields;
- (4) Perform one time-step SFD-DEOM evolution with Eq. (23);
- (5) Repeat Steps (1)–(4) to generate one trajectory  $\tilde{\rho}_s(t; \tilde{\xi}_t, \tilde{\xi}'_t)$ ;

- (6) Repeat Step (5) to generate multiple trajectories;
- (7) Evaluate the ensemble average until convergence via Eq. (24).

The inverted expression of  $\xi_t$  and  $\xi'_t$  depending on  $\{\tilde{\xi}_\tau; \tau \leq t\}$  and  $\{\tilde{\xi}'_\tau; \tau \leq t\}$  can not be explicitly written due to Eq. (29) with Eq. (30). Norm-conserving and non-norm-conserving (without the GT step) schemes can only be compared numerically and will be demonstrated in Sec. III.

### III. NUMERICAL DEMONSTRATIONS

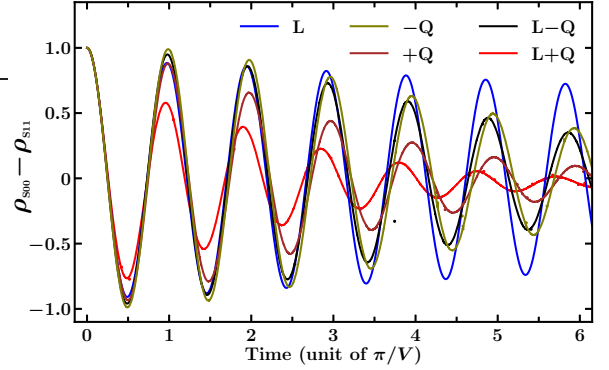


FIG. 1: Population evolutions of two-state dissipative systems under different bath coupling cases. See the main text for the model and parameter details.

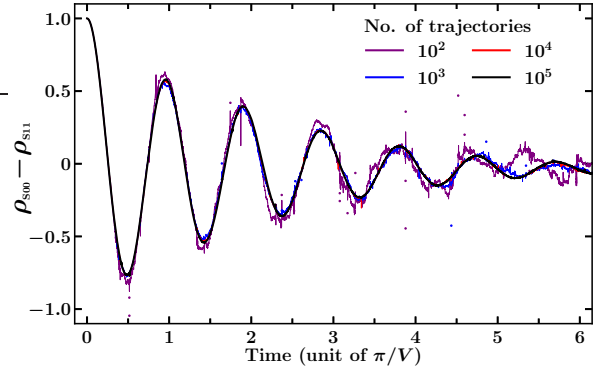


FIG. 2: Time evolutions versus number of trajectories towards convergence of the “L+Q”-case simulation in Fig. 1.

For numerical demonstrations, we select a two-state model system as in Ref. 26. The model, corresponding to the form of Eq. (1), can be recast here as

$$H_s = \omega_{10}|1\rangle\langle 1| + V(|1\rangle\langle 0| + |0\rangle\langle 1|) \text{ and } \hat{Q}_s = |1\rangle\langle 1|. \quad (34)$$

This corresponds to the initial state being at  $|0\rangle$  equilibrated with the solvent before the transfer- $V$ -action triggered. Under some basic physical considerations, elaborations in Ref. 26 give that the  $\{\alpha_0, \alpha_1, \alpha_2\}$ -descriptors, which indicate the bath coupling strengths, are related

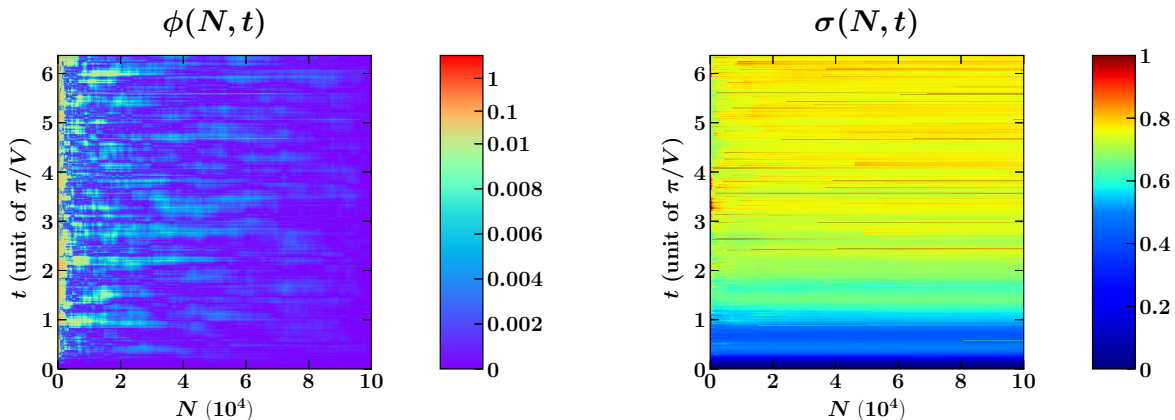


FIG. 3: Contour plots to exhibit the convergence behaviors of average and variance versus the number of sampling trajectories  $N$  and time  $t$ ,  $\phi(N, t)$  (left-panel) and  $\sigma(N, t)$  (right-panel), respectively, exemplified with the “L+Q”-case simulation in Fig. 1. The contour coloring of the left panel uses a mixed logarithmic-rectangular scheme. See the main text for the definitions of  $\phi(N, t)$  and  $\sigma(N, t)$ .

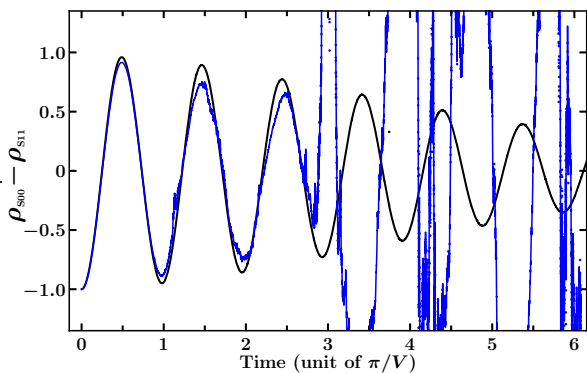


FIG. 4: Comparison between norm-conserving (in black) and non-norm-conserving (in blue) calculations of Fig. 1’s “L+Q”-case upon  $4 \times 10^4$  trajectories. The blue one diverges heavily.

with a parameter  $\theta_B \equiv \omega'_B/\omega_B$ . Here,  $\omega'_B$  and  $\omega_B$  are the characteristic solvation-mode frequencies according to the system being at  $|1\rangle$  and  $|0\rangle$  states, respectively. We choose the Brownian-oscillator solvent model

$$J_B(\omega) = \frac{\zeta \omega_B \omega}{(\omega_B^2 - \omega^2)^2 + (\zeta \omega)^2}. \quad (35)$$

The  $\{\alpha_n\} \sim \theta_B$  relations for this model are given as[26]

$$\alpha_0 = \lambda \theta_B^2, \quad \alpha_1 = -(2\lambda \omega_B)^{\frac{1}{2}} \theta_B^2, \quad \alpha_2 = \frac{\omega_B}{2} (\theta_B^2 - 1). \quad (36)$$

Here,  $\lambda$  is the linear-displacement induced reorganization.

In the following demonstrations,  $k_B T$  is set as the unit of energy and reciprocal of time. The other parameters are chosen as  $\omega_{10} = 0$  and  $V = \omega_B = \zeta = 1$ ;  $\lambda = 0.1$  or 0 for with or without linear terms; and  $\theta_B = 0.8, 1, 1.25$  for different quadratic coupling cases. Exhibited in Fig. 1 are for five conditions: (i) pure linear-bath-coupling (L) with  $\lambda = 0.1$  and  $\theta_B = 1$  resulting in  $\{\alpha_0, \alpha_1, \alpha_2\} = \{0.1, -0.45, 0\}$ ; (ii) pure negative-sign ( $\theta_B < 1$ ) quadratic-bath-coupling (-Q) with  $\lambda = 0$

and  $\theta_B = 0.8$  resulting in  $\{\alpha_0, \alpha_1, \alpha_2\} = \{0, 0, -0.18\}$ ; (iii) pure positive-sign ( $\theta_B > 1$ ) quadratic-bath-coupling (+Q) with  $\lambda = 0$  and  $\theta_B = 1.25$  resulting in  $\{\alpha_0, \alpha_1, \alpha_2\} = \{0, 0, 0.28\}$ ; (iv) L-Q with  $\lambda = 0.1$  and  $\theta_B = 0.8$  resulting in  $\{\alpha_0, \alpha_1, \alpha_2\} = \{0.064, -0.29, -0.18\}$ ; and (v) L+Q with  $\lambda = 0.1$  and  $\theta_B = 1.25$  resulting in  $\{\alpha_0, \alpha_1, \alpha_2\} = \{0.16, -0.7, 0.28\}$ . Apparently, for case (i), SFD-DEOM is just reduced to original DEOM with no stochastic field involved. For each of the other four cases, (ii)-(v),  $10^5$  trajectories have been sampled. Time step is set as  $\Delta t = 0.001$  in the unit of  $(k_B T)^{-1}$ . Computing results versus number of trajectories towards convergence is illustrated in Fig. 2, exemplified with the case (v) of “L+Q”. We can see that results from  $10^4$  (red) and  $10^5$  (black) trajectories almost coincide, and that of  $10^3$  (blue) trajectories is very close to them apart from some serration.

We may also be interested in the numerical convergence of average and variance versus the number of sampling trajectories. Denote

$$P(N, t) \equiv \langle \rho_{s00}(t) - \rho_{s11}(t) \rangle_N,$$

specifying that the average is over  $N$  trajectories. Its variance is then defined as

$$\sigma(N, t) \equiv \langle [\rho_{s00}(t) - \rho_{s11}(t) - P(N, t)]^2 \rangle_N^{1/2}.$$

Introduce  $\phi(N, t) \equiv |P(N, t) - P(N_{\max}, t)|$  to show the convergence of average, where  $N_{\max} = 10^5$  is the maximum number of trajectories in our computation.  $\phi(N, t)$  and  $\sigma(N, t)$  are exhibited in the left and right panels of Fig. 3, respectively. The right panel of Fig. 3 demonstrates that the variance grows with  $t$ . For the convergence of average, the left panel of Fig. 3 indicates that more trajectories are needed for longer  $t$  simulations. The oscillating behaviors in both panels should be caused according to the oscillation of population evolution.

The norm conservation via GT is necessary to greatly improve the sampling efficiency and simulating stability.

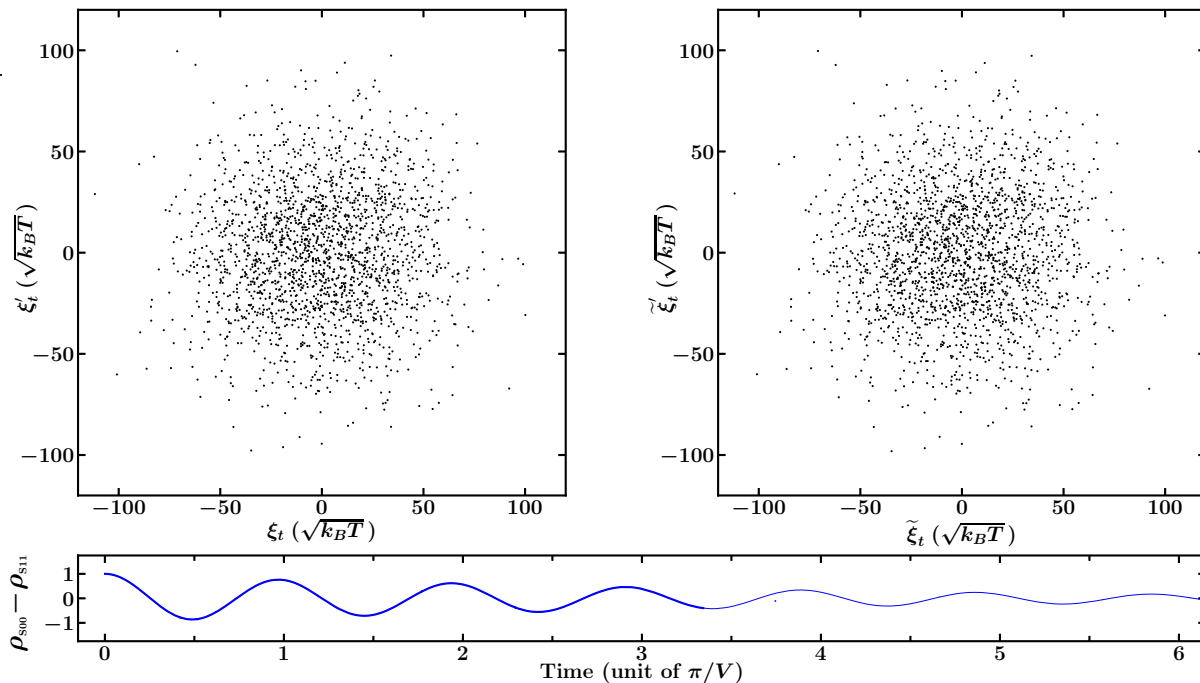


FIG. 5: Stochastic fields before and after GT, i.e.,  $(\xi_t, \xi'_t)$  versus  $(\tilde{\xi}_t, \tilde{\xi}'_t)$ , with the time  $t$  corresponding to the evolution progress bar indicated in the lower panel of Fig. 1’s “L–Q”-case. Points in the upper panels are drawn upon 2000 sampled trajectories from Fig. 4. (Multimedia view)

Non-norm-conserving calculations without adopting GT are found very hardly converged, for the cases we have tested. The divergence of non-norm-conserving calculation is exemplified in Fig. 4 with the case (iv) of “L–Q” for the comparison between norm-conserving (in black) and non-norm-conserving (in blue) schemes, upon  $4 \times 10^4$  trajectories. During the earlier period before the blue one diverges, there is still small difference between two results. Besides the possible reason that the black curve is converged result while the blue one not yet, the difference may also be caused due to that GT is only accurate in the limit  $\Delta t \rightarrow 0$  but now it is  $\Delta t = 0.001$  in the unit of  $(k_B T)^{-1}$ . We exhibit in Fig. 5 (Multimedia view) the stochastic fields,  $(\xi_t, \xi'_t)$  versus  $(\tilde{\xi}_t, \tilde{\xi}'_t)$ , drawn upon 2000 sampled trajectories from the calculations of Fig. 4. In overall speaking, the two pairs of stochastic fields, before and after GT, are seen to be of similar distribution with the distribution width about  $1/\sqrt{\Delta t} \approx 30\sqrt{k_B T}$ . Thus the GT actually does not alter the basic statistical properties of stochastic fields, but the involved norm conservation treatment constitutes the crucial step to successfully carry out the SFD–DEOM simulations.

#### IV. SUMMARY

In summary, we propose a stochastic-fields-dressed dissipaton-equation-of-motion (SFD–DEOM) method to tackle the nonlinear coupling bath effects. The stochastic fields are introduced via the Hubbard–Stratonovich (HS) transformation just for the nonlinear bath coupling components. After the HS transforma-

tion, the total Hamiltonian is converted to the common linear bath coupling form and DEOM can then be constructed under the stochastic dressing fields. Originally, dissipatons are quasi-particles characterizing the statistical effects of linear coupling Gaussian bath. The stochastic fields promote them to treat further nonlinear bath couplings. With the ensemble average over these fields, the SFD–DEOM provides an exact and nonperturbative approach to quantum dissipation under nonlinear bath couplings. Although the paper is exemplified just with quadratic bath couplings, the SFD–DEOM method can be systematically generalized to higher-order bath couplings via multiple HS transformations. It can also serve as a basis for further development of other practical simulation methods toward realistic molecular systems in condensed phases.

#### Acknowledgments

Support from the Ministry of Science and Technology of China, Grant No. 2017YFA0204904, and the National Natural Science Foundation of China, Nos. 21633006, 22103073, and 22173088 is gratefully acknowledged. Wang Y and Chen ZH thank also the partial support from GHfund B (20210702).

**Data Availability:** The data that support the findings of this study are available from the corresponding author upon reasonable request.

- 
- [1] R. P. Feynman and F. L. Vernon, Jr., “The theory of a general quantum system interacting with a linear dissipative system,” *Ann. Phys.* **24**, 118 (1963).
- [2] H. Kleinert, *Path Integrals in Quantum Mechanics, Statistics, Polymer Physics, and Financial Markets*, World Scientific, Singapore, 2009, 5<sup>th</sup> ed.
- [3] U. Weiss, *Quantum Dissipative Systems*, World Scientific, Singapore, 2012, 4<sup>th</sup> ed.
- [4] Y. Tanimura and R. Kubo, “Time evolution of a quantum system in contact with a nearly Gaussian-Markovian noise bath,” *J. Phys. Soc. Jpn.* **58**, 101 (1989).
- [5] Y. A. Yan, F. Yang, Y. Liu, and J. S. Shao, “Hierarchical approach based on stochastic decoupling to dissipative systems,” *Chem. Phys. Lett.* **395**, 216 (2004).
- [6] A. Ishizaki and Y. Tanimura, “Quantum dynamics of system strongly coupled to low temperature colored noise bath: Reduced hierarchy equations approach,” *J. Phys. Soc. Jpn.* **74**, 3131 (2005).
- [7] R. X. Xu, P. Cui, X. Q. Li, Y. Mo, and Y. J. Yan, “Exact quantum master equation via the calculus on path integrals,” *J. Chem. Phys.* **122**, 041103 (2005).
- [8] Y. Tanimura, “Numerically “exact” approach to open quantum dynamics: The hierarchical equations of motion (HEOM),” *J. Chem. Phys.* **153**, 020901 (2020).
- [9] Y. J. Yan, “Theory of open quantum systems with bath of electrons and phonons and spins: Many-dissipaton density matrixes approach,” *J. Chem. Phys.* **140**, 054105 (2014).
- [10] R. X. Xu, H. D. Zhang, X. Zheng, and Y. J. Yan, “Dissipaton equation of motion for system-and-bath interference dynamics,” *Sci. China Chem.* **58**, 1816 (2015), Special Issue: Lemin Li Festschrift.
- [11] H. D. Zhang, R. X. Xu, X. Zheng, and Y. J. Yan, “Statistical quasi-particle theory for open quantum systems,” *Mol. Phys.* **116**, 780 (2018), Special Issue, “Molecular Physics in China”.
- [12] Y. Wang, R. X. Xu, and Y. J. Yan, “Entangled system-and-environment dynamics: Phase-space dissipaton theory,” *J. Chem. Phys.* **152**, 041102 (2020).
- [13] H. D. Zhang, R. X. Xu, X. Zheng, and Y. J. Yan, “Non-perturbative spin-boson and spin-spin dynamics and nonlinear Fano interferences: A unified dissipaton theory based study,” *J. Chem. Phys.* **142**, 024112 (2015).
- [14] Z.-H. Chen, Y. Wang, R.-X. Xu, and Y. Yan, “Correlated vibration–solvent effects on the non-Condon exciton spectroscopy,” *J. Chem. Phys.* **154**, 244105 (2021).
- [15] D. Vion, A. Aassime, A. Cottet, P. Joyez, H. Pothier, C. Urbina, D. Esteve, and M. H. Devoret, “Manipulating the quantum state of an electrical circuit,” *Science* **296**, 886 (2002).
- [16] Y. Makhlin and A. Shnirman, “Dephasing of solid-state qubits at optimal points,” *Phys. Rev. Lett.* **92**, 178301 (2004).
- [17] E. A. Muljarov and R. Zimmermann, “Dephasing in quantum dots: Quadratic coupling to acoustic phonons,” *Phys. Rev. Lett.* **93**, 237401 (2004).
- [18] P. Bertet, I. Chiorescu, G. Burkard, K. Semba, C. J. P. M. Harmans, D. P. DiVincenzo, and J. E. Mooij, “Dephasing of a superconducting qubit induced by photon noise,” *Phys. Rev. Lett.* **95**, 257002 (2005).
- [19] Y. J. Yan and S. Mukamel, “Eigenstate-free, Green function: Calculation of molecular absorption and fluorescence line shapes,” *J. Chem. Phys.* **85**, 5908 (1986).
- [20] Q. Peng, Y. P. Yi, Z. G. Shuai, and J. S. Shao, “Excited state radiationless decay process with Duschinsky rotation effect: formalism and implementation,” *J. Chem. Phys.* **136**, 114302 (2007).
- [21] H. Wang and M. Thoss, “Quantum Dynamical Simulation of Electron-Transfer Reactions in an Anharmonic Environment,” *J. Phys. Chem. A* **111**, 10369 (2007).
- [22] Y. Zhao and W. Z. Liang, “Charge transfer in organic molecules for solar cells: theoretical perspective,” *Chem. Soc. Rev.* **41**, 1075 (2012).
- [23] V. Chorošajev, T. Marčiulionis, and D. Abramavicius, “Temporal dynamics of excitonic states with nonlinear electron-vibrational coupling,” *J. Chem. Phys.* **147**, 074114 (2017).
- [24] Y. Wang, Y. Su, R. X. Xu, X. Zheng, and Y. J. Yan, “Marcus’ electron transfer rate revisited via a generalized Rice–Ramsperger–Kassel–Marcus theory with nonlinear environments,” *Chin. J. Chem. Phys.* **34**, 462 (2021).
- [25] R. X. Xu, Y. Liu, H. D. Zhang, and Y. J. Yan, “Theory of quantum dissipation in a class of non-Gaussian environments,” *Chin. J. Chem. Phys.* **30**, 395 (2017).
- [26] R. X. Xu, Y. Liu, H. D. Zhang, and Y. J. Yan, “Theories of quantum dissipation and nonlinear coupling bath descriptors,” *J. Chem. Phys.* **148**, 114103 (2018).
- [27] Y. A. Yan, “Stochastic simulation of anharmonic dissipation. II. Harmonic bath potentials with quadratic couplings,” *J. Chem. Phys.* **150**, 074106 (2019).
- [28] C. Hsieh and J. Cao, “A unified stochastic formulation of dissipative quantum dynamics. II. Beyond linear response of spin baths,” *J. Chem. Phys.* **148**, 014104 (2018).
- [29] J. T. Hsiang and B. L. Hu, “Nonequilibrium nonlinear open quantum systems: Functional perturbative analysis of a weakly anharmonic oscillator,” *Phys. Rev. D* **101**, 125002 (2020).
- [30] J. T. Hsiang and B. L. Hu, “Fluctuation-dissipation relation from the nonequilibrium dynamics of a nonlinear open quantum system,” *Phys. Rev. D* **101**, 125003 (2020).
- [31] R. L. Stratonovich, “On a Method of Calculating Quantum Distribution Functions,” *Dokl. Akad. Nauk S.S.S.R* **115**, 1097 (1957).
- [32] J. Hubbard, “Calculation of Partition Functions,” *Phys. Rev. Lett.* **3**, 77 (1959).
- [33] J. S. Shao, “Decoupling quantum dissipation interaction via stochastic fields,” *J. Chem. Phys.* **120**, 5053 (2004).
- [34] B. Øksendal, *Stochastic Differential Equations*, Springer, Berlin, 2005, 6<sup>th</sup> ed.
- [35] G. C. Ghirardi, P. Pearle, and A. Rimini, “Markov processes in Hilbert space and continuous spontaneous localization of systems of identical particles,” *Phys. Rev. A* **42**, 78 (1990).
- [36] D. Gatarek and N. Gisin, “Continuous quantum jumps and infinite-dimensional stochastic equations,” *J. Math. Phys.* **32**, 2152 (1991).